



CHARACTERIZATION OF MAGNETIC MINERALS OF IRON SAND PASIA NAN TIGO PADANG BEACH USING X-RAY DIFFRACTION (XRD)

Ardilla Nofri Yuwanda, Riza Rahmayuni, Dwi Anisa Visgun, Annisa rahmi, Hamdi Rifai* dan Letmi Dwiridal

Department of Physics, FMIPA, Universitas Negeri Padang, Padang, Indonesia
* rifai.hamdi@fmipa.unp.ac.id

Received 27-05-2021, Revised 21-02-2022, Accepted 22-02-2022
Available Online 17-03-2022, Published Regularly April 2022

ABSTRACT

The mineral extraction of iron sand from Pasia Nan Tigo Beach has been carried out. Iron sands in this area are widely spread and have decent potential but have not been used optimally. The iron sand of Pasia Nan Tigo Beach contains minerals that are indicated by the variation in susceptibility values of type $265.8 \times 10^{-8} \text{ m}^3/\text{kg}$ to $12,445.53 \times 10^{-8} \text{ m}^3/\text{kg}$. Therefore, it is necessary to separate minerals from iron sand so that the minerals contained in them are known so that they are suitable for usability. The iron sand obtained is extracted using two magnets, namely a strong magnet and a weak magnet. The extraction results from iron sand still contain impurities to remove them, the sand is purified and then the sand extraction results are characterized using the XRD method. Content The type and structure of the mineral species found in the samples extracted from iron sand using strong magnets are Magnetite (Fe_3O_4) with Cubic structure, Hematite ($\alpha\text{-Fe}_2\text{O}_3$) with Hexagonal structure, and Ilmenite (FeTiO_3) with Hexagonal structure. While the use of weak magnets is Magnetite (Fe_3O_4) with Cubic structure, Hematite ($\alpha\text{-Fe}_2\text{O}_3$) with Rhombohedral structure, and Ilmenite (FeTiO_3) with Rhombohedral structure. Meanwhile, the non-magnetic mineral namely Quartz (SiO_2), works as an impurity. The average crystal size using a strong magnet for PNT-B01 0-5 cm is 100.85 nm and a weak magnet is 49.36 nm, sample A06 30-35 cm uses a strong magnet of 88.25 nm and a weak magnet of 46, 80 nm, meanwhile sample B10 0-5 cm with a strong magnet of 109.22 nm and a weak magnet of 45.60 nm.

Keywords: extraction; magnetic minerals; iron sand; crystal size; pasia nan tigo.

INTRODUCTION

Natural resources abound in Indonesia. Indonesia has a tectonic layout that supports its potential natural resources, such as large mineral mines, due to geological conditions^[1]. Iron Sand is one of Indonesia's mineral mines, and it may be found across the country, including along the southern coast of Java, West Nusa Tenggara, and Sumatra^[2]. West Sumatra is one of the provinces with the highest potential for iron sand, but it has yet to be completely utilized^[3] Pasia Nan Tigo Beach is one of those. Pasia Nan Tigo Beach is a sloping and sandy beach in Padang City's Koto Tengah sub-district. It is composed of grayish-brown sand with coarse granules^[4]. This area has a bunch of iron sand, which has a lot of potential and economic value. The material (rock, sand, gravel) is carried away from the river and sedimented due to the passage of seawater, and the material is distributed to the coast continuously for a long time, resulting in the addition of iron sand deposits.

The mineral content of iron sand is generally present in metal oxides [5]. Sand contains a lot of iron, titanium, silica, and other elements [6,7]. The minerals have 88% magnetic and 12% non-magnetic [8]. Minerals having high magnetic characteristics are known as magnetic minerals [9], Iron magnetite (Fe_3O_4), hematite ($\alpha\text{-Fe}_2\text{O}_3$), and maghemite ($\beta\text{-Fe}_2\text{O}_3$) are the most abundant minerals in the sand, and they have industrial applications as a mixed dye (filler) for paints and as a base material for permanent magnets. Magnetite is a mineral that is used as a base for dry ink or toner [10], laser printers, magnetite nanoparticles as biomedical applications [11] and anti-cancer [12,13], the manufacture of ferrous metal [5]. Minerals Hematite can also be used as a major component in the manufacture of photoelectrochemical solar cells [14], manufacture of magnets [15], raw materials for lithium batteries [16], and industrial materials based on magnetism [17]. The magnetic mineral content of iron sand is very large, especially on Pasia Nan Tigo Beach, so it cannot be utilized optimally [2].

Material can be determined by its magnetic properties by measuring its magnetic susceptibility value [18-22]. One thing that affects the susceptibility value is Fe which has ferromagnetic properties. Beach sand Pasia Nan Tigo iron-containing magnetic minerals as indicated by the variation in magnetic susceptibility $1,303.57 \times 10^{-8} \text{m}^3/\text{kg}$, $2,882.43 \times 10^{-8} \text{m}^3/\text{kg}$, and $12,445.53 \times 10^{-8} \text{m}^3/\text{kg}$. Therefore, it is necessary to separate the minerals from iron sand to make it more efficient. The extraction process is carried out using manual extraction or using permanent magnets with several draws [23,24] with the percentage of magnetic mineral content drawn using a strong magnet, namely 58.7%, 80.9%, and 31.70% while using a weak magnet of 15.5%, 2.62%, and 4.09% and further characterized using X-Ray Diffraction (XRD).

METHODS

This research includes sampling, sample preparation, extraction of iron sand samples, measurements using XRD, data analysis, and interpretation. Sampling was carried out at a location between $00^\circ 17,974' - 00^\circ 64,961'$ South latitude and $100^\circ 19,791' - 100^\circ 31,850'$ East Longitude which is located in Pantai Pasia Nan Tigo, Koto Tangah District, Padang City which stretches 7.2 km and divided into three regions (Pasia Jambak, Pasia Kandang, and Pasia Sabalah). Around this area, there are estuaries where the river and sea meet, namely Muaro Anai, Muaro Baru, and Muaro Panjalinan (Figure 1). The coastal area of Pasia Nan Tigo is located at an altitude of 0–3 meters above sea level, the width of the beach ranges from 2 to 21 meters and the slope of 0–2% causes this village to be classified as lowland [25]. Therefore, Pasia Nan Tigo Beach is a sloping and sandy beach. The sand in this area consists of sand that is grayish brown with coarse grains [4].

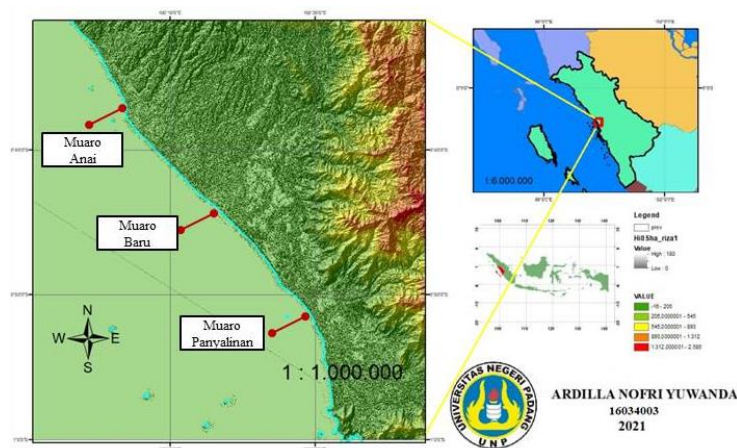


Figure 1. Locations of Sampling on a Map

Furthermore, iron sand extraction is used to separate magnetic and non-magnetic materials during the separation process. The following is the magnetic mineral extraction process for iron sand:

- 1) Strong magnets and weak magnets are being used to extract iron sand samples that have already been dried and weighed up to 100 grams (Figure 2). The process to extract material from a mixture is called extraction ^[26]. The separation of magnetic minerals from the sources is also known as iron sand magnetic mineral extraction. Extraction using a strong magnet aims to separate sand containing Fe and other than Fe while using a weak magnet aims to make the iron sand attracted by the magnet have strong magnetic or magnetic properties.

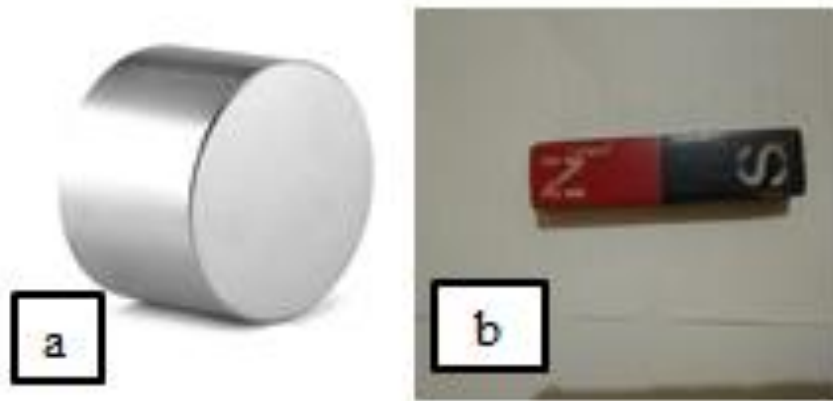


Figure 2. Permanent magnets are used for magnetic mineral extraction (a) Strong Magnets, (b) Weak Magnets

- 2) Furthermore, iron sand extraction is done both with strong and weak magnets by extracting a sample with a strong magnet that has a pull of up to 20 times the pull of a weak magnet. Semua mineral magnet, baik yang magnetnya lemah maupun yang magnetnya kuat, mengandung efek tarikan dengan magnet yang kuat. magnet yang lemah menarik pasir besi yang telah ditarik kembali oleh magnet yang kuat. As a result, iron sand is obtained, which has a stronger magnet and looks blacker in color, whereas the remainder of the withdrawal using a strong magnet looks brownish and the sand's magnetism is no longer visible (Figure 3).

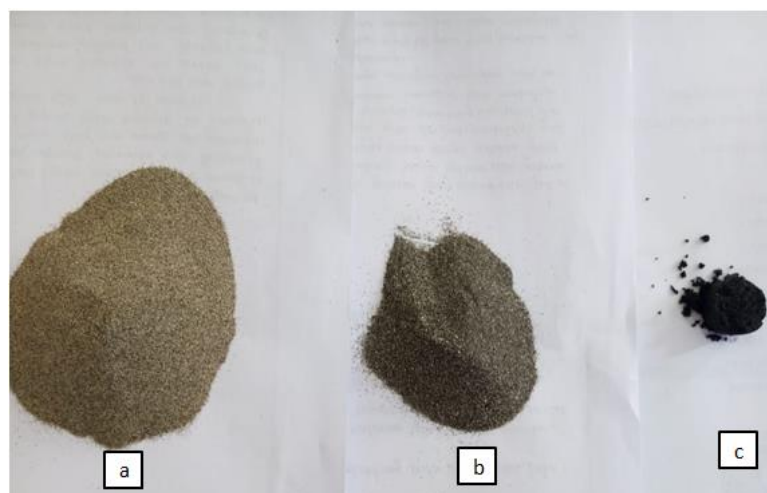


Figure 3. Results of extraction of iron sand (a) remaining withdrawal of iron sand, (b) results of withdrawal with Strong Magnets, (c) results of withdrawals with Weak Magnets

- 3) Other impurities are still contained in the magnetic minerals that are attracted by the magnet. As a result, the samples were cleaned with Aquadest in an Ultrasonic Cleaner BK-1200. Ultrasonic Cleaner uses ultrasonic waves to create vibrations that easily remove impurities from magnetic minerals.
- 4) The sample is then dried once it has been washed.
- 5) After drying, the sample is placed in a holder and brought to the Material Physics Laboratory, Department of Physics, FMIPA, Padang State University, where it is analyzed using a PANalytical X Pert Pro PW 3060/10 XRD with a Pixel 1-D type detector to determine the mineral type. (Figure 4).

By comparing measured data to mineral databases, XRD is used to determine mineral types. While for the crystalline phase in a material it was carried out with lattice parameters and the diffraction pattern found at a certain peak angle was characteristic of a sample. The crystal size can be determined using the equation Debye Scherrer^[27].

$$D = K \frac{\lambda}{B \cos \theta_B} \quad (1)$$

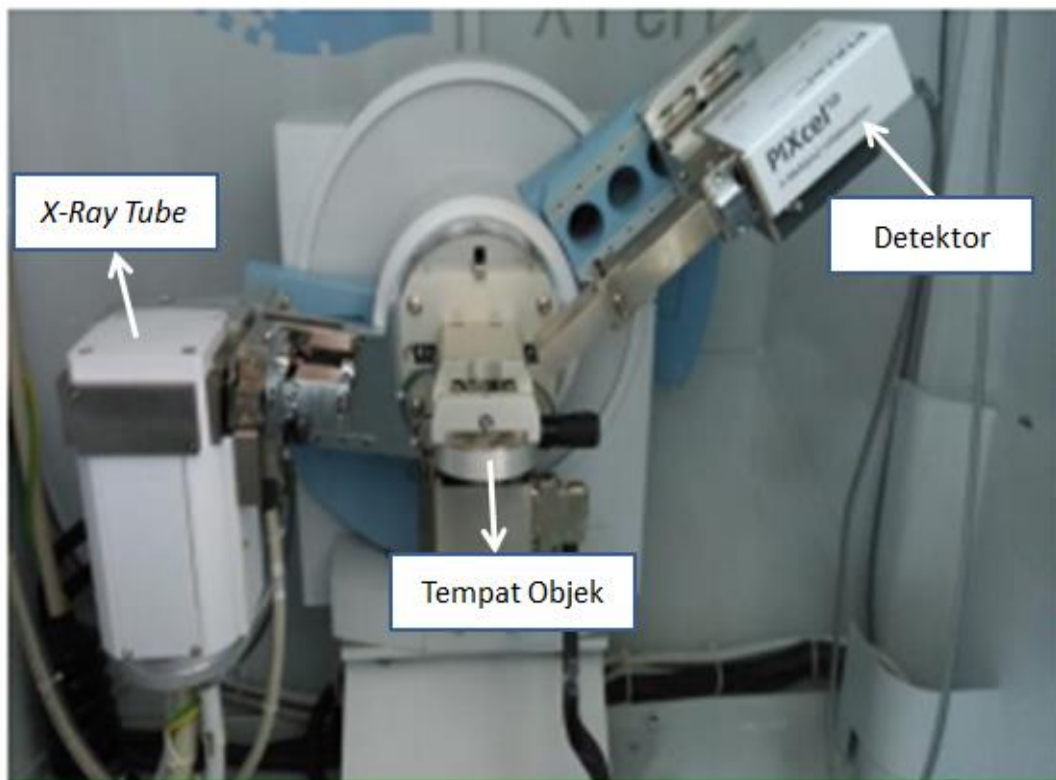


Figure 4. The main part of the *X-Ray Diffractometer (XRD)*

RESULTS AND DISCUSSION

1. Permanent magnets were used to determine the proportion of magnetic mineral concentration in iron sand.

Table 1 shows that iron sand in Pasia Nan Tigo Village has different magnetic mineral content percentages. After separation using strong magnets, iron sand from the PNT20-0616-

1-A06 sample at a depth of 30-35 cm was more attracted than the PNT20-0616-1-B01 cm and PNT20-0616-1-B10 samples at a depth of 0-5 cm. Meanwhile, using a weak magnet has a percentage of the magnetic mineral content of 15.55%, 2.62%, and 4.09%. Of the three coastal sampling locations, Pasia Jambak has a high percentage of magnetic mineral content for weak magnetic drawing compared to other sample locations.

Table 1. Pasia Nan Tigo's magnetic mineral composition as a percentage after being extracted using strong and weak magnets.

No	Location Sample	Name sample	Susceptibility (10^{-8} m ³ / kg)	Magnets Strong		Weak		Magnets Remaining Strong- Weak Magnets
				Mass (gram)	(%)	Mass (gram)	(%)	
1	Pasia Jambak	PNT20-0616- 1-B01 0-5 cm	12,445,533	58.79	58.79	15.55	15.55	25.66
2	Pasia Sabalah	PNT20-0616- 1-A06 30-35 cm	1,303,567	80.92	80.92	2.61	2.62	16.46
3	Pasia Kandang	PNT20-0616- 1-B10 0-5 cm	2,882.433	31.7	31.7	4,096	4.09	64.21

2. Data measurement Results sample results from iron sand extraction with XRD

measurement results for sample extraction of iron ore by XRD as a function of diffraction intensity diffraction angle (2θ). The measurement data is obtained in the form of a graphic called a diffractogram. Analysis of the diffractogram was carried out to obtain the type of mineral, crystal structure, and crystal size. The mineral type is shown by comparing the angle of diffraction (2θ), relative intensity(I_r) of the measurement results with the database mineral.

a. PNT20-0616-1-B01 0-5 cm

1) Measurement data of iron sand extraction samples using strong and weak magnets

The samples from the iron sand extraction of PNT area sample B01 were measured using XRD at a depth of 0-5 cm. Mineral kinds are recognized using the diffraction angle (2θ), and the distance of fields (d), with magnetic and non-magnetic minerals being recognized by comparing measurement techniques such as data mineral database.

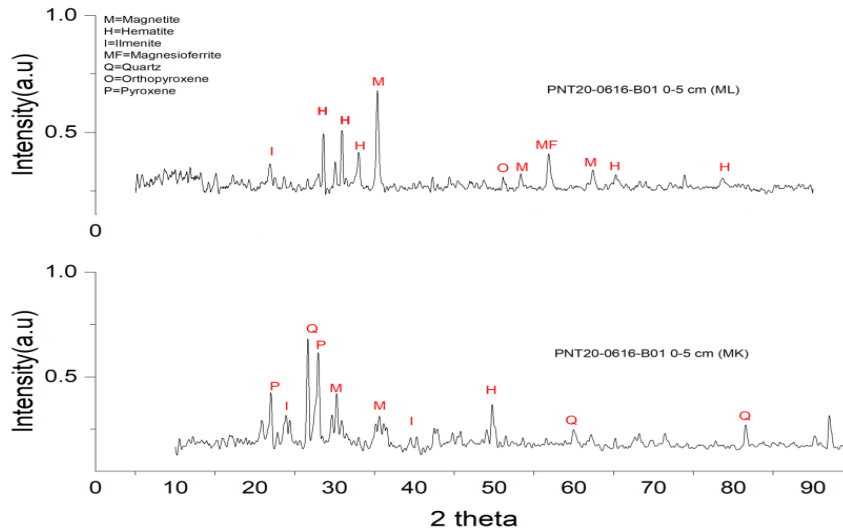


Figure 5. the results of XRD measurements of samples of iron sands extraction uses powerful magnets and a weak magnetic PNT region at a depth of 0-5 cm

Table 2. Comparison of measurement data with a database of mineral samples of iron sands extraction uses powerful magnets.

Measurement data			Mineral Database			Type of mineral	Crystal System	D (nm)
2θ(°)	d[Å]	I _r (%)	2θ(°)	d[Å]	I _r (%)			
22.019	4.037	52.14	22.031	4.031	0.0	Pyroxene	Orthorhombic	126.57
23.955	3.715	38.56	23.913	3.718	32.3	Ilmenite	Rhombohedral	211.51
26.662	3.344	95.07	26.624	3.345	100.0	Quartz	Hexagonal	106.38
27.949	3.192	100	27.810	3.205	21.6	Pyroxene	Orthorhombic	128.03
30.244	2.955	41.47	30.664	2.913	28.2	Magnetite	Cubic	80.41
35.143	2.554	24.33	35.111	2.554	100.0	Magnesioferrite	Cubic	108.58
36.158	2.484	25.06	36.124	2.484	100.0	Magnetite	Cubic	108.89
40.350	2.235	5.89	40.477	2.227	16.7	Ilmenite	Rhombohedral	55.14
49.740	1.833	29.02	49.533	1.839	42.1	Hematite	Rhombohedral	85.55
60.102	1.540	9.11	59.926	1.542	6.3	Quartz	Hexagonal	29.89
81.582	1.180	15.2	81.440	1.181	1.5	Quartz	Hexagonal	68.35

Table 3. Comparison of measurement data with databases mineral of samples extracted from iron sand that is drawn using a weak magnet.

Measurement data			Mineral Database			Types of minerals	Crystal System	D (nm)
2θ(°)	d[Å]	I _r (%)	2θ(°)	d[Å]	I _r (%)			
23.700	3.756	9.6	23.847	3.728	23.4	Ilmenite	Rhombohedral	52.88
27.909	3.197	17.3	27.895	3.196	100.0	Hematite	Rhombohedral	53.33
31.022	2.888	36.1	31.200	2.859	15.9	Hematite	Rhombohedral	26.85
33.012	2.713	35.7	33.099	2.704	100.0	Hematite	Rhombohedral	53.98
35.365	2.538	100.0	35.455	2.530	100.0	Magnetite	Cubic	54.32
51.165	1.785	10.6	51.174	1.798	3.6	Orthopyroxene	Orthorhombic	34.42
53.357	1.717	13.0	53.456	1.713	9.2	Magnetite	Cubic	57.92
56.840	1.619	35.7	56.837	1.619	31.0	Magnesioferrite	Cubic	58.84
62.381	1.489	19.1	62.390	1.487	24.2	Hematite	Rhombohedral	60.47
65.469	1.426	5.1	65.570	1.415	0.2	Hematite	Rhombohedral	23.07
78.617	1.217	8.7	78.745	1.214	0.9	Hematite	Rhombohedral	66.87

At an angle of 2θ with a peak of 30.400° , and 36.158° , XRD tests in the PNT20-0616-1-B01 sample at a depth of 0-5 cm using a strong magnet (Table 2) indicate the type of magnetic minerals present, namely Magnetite^[28,29], Hematite is obtained at a diffraction angle of 2θ with a peak of 49.640° and Ilmenite is obtained at a diffraction angle of 23.955° , and 40.350° . Other mineral types are Magnesioferrite, which has a diffraction angle of 35.143° , and Quartz a non-magnetic mineral which has diffraction angles of 2θ 26.662° , 60.102° , and 81.582° with the most significant intensity reaching 100%. The diffractogram analysis reveals that magnetite (Fe_3O_4), hematite ($\alpha\text{-Fe}_2\text{O}_3$), and ilmenite (FeTiO_3) are the minerals that make it up to iron sand. Because many non-magnetic minerals, such as Quartz and Pyroxene, are still identified from XRD measurements, iron sand extraction was performed using a weak magnet to obtain magnetic minerals.

Lattice parameters mineral Magnetite with $a=b=c=8.240.0 \text{ \AA}$; $\alpha=\beta=\gamma=90^\circ$ as well as the relative intensity derived from the measurements for minerals Magnetite is 41.47% and 25.06%. Hematite has lattice parameters $a=b=5.068 \text{ \AA}$, $c=13.996 \text{ \AA}$; $\alpha=\beta=90^\circ$ and $\gamma=120^\circ$ with the space group R-3c having a Hexagonal structure. Meanwhile, Ilmenite has lattice parameters $a=b=5.028 \text{ \AA}$, $c=13.730 \text{ \AA}$; $\alpha=\beta=90^\circ$ and $\gamma=120^\circ$ with the space group R-3 having a Hexagonal structure.

The obtained diffractogram analysis (Table 3), the magnetic minerals that makeup iron sand are known at the diffraction angle with peaks (2θ) of 35.365° , and 53.357° which are minerals Magnetite (Fe_3O_4) with a distance between d [\AA] of planes $2.538.1 \text{ \AA}$, and 1.717 \AA with lattice parameters $a=b=c= 8.390.4 \text{ \AA}$; $\alpha=\beta= \gamma=90^\circ$, while at the diffraction angle 2θ with peaks of 27.909° , 31.022° , 33.012° , 62.381° , 65.469° , and 78.617° the known minerals are Hematite ($\alpha\text{-Fe}_2\text{O}_3$) with lattice parameters $a=b=5.036 \text{ \AA}$ and $c=13.787 \text{ \AA}$; $\alpha=\beta= 90^\circ$ and $\gamma=90^\circ$ with the space group R-3c having a Rhombohedral structure. Meanwhile, Ilmenite (FeTiO_3) is known to occur in diffraction angle 2θ with a peak of 23.700° with lattice parameters $a=b= 5.083 \text{ \AA}$ and $c=14.026 \text{ \AA}$; $\alpha=\beta=90^\circ$ and $\gamma=120^\circ$ with the space group R-3 having a Rhombohedral structure. Strong magnets had an average crystal size of 100.85 nm, while weak magnets had an average crystal size of 49.36 nm. Weak magnetic extraction also obtained non-magnetic minerals, namely Ortopyroxene, but the dominant magnetic minerals were obtained, namely Magnetite, Hematite, Magnesioferrite, and Ilmenite.

b. PNT20-0616-1-A06 30-35

1) Measurement data of iron sand extraction samples using strong and weak magnets

The samples from the iron sand extraction of PNT area sample B01 were measured using XRD at a depth of 0-5 cm, yielding a diffractogram (Figure 6) with some peaks visible. Mineral kinds are recognized using the diffraction angle (2θ), and the distance of fields (d), with magnetic and non-magnetic minerals being recognized by comparing measurement techniques such as data mineral database (Tables 4 and 5).

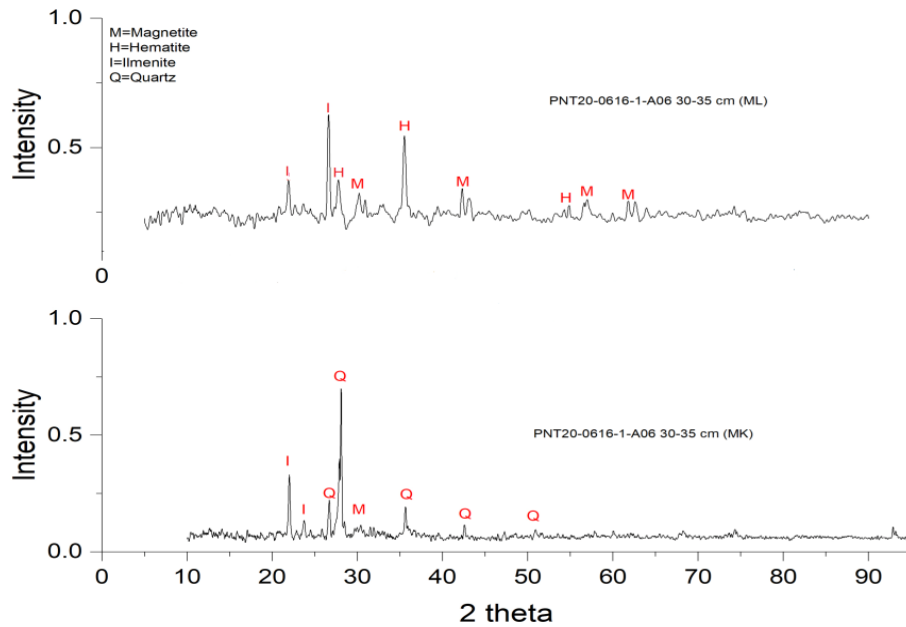


Figure 6. Measurement results of XRD samples extracted from iron sand using strong and weak magnets in the PNT region at a depth of 30-35 cm

Table 4. Comparison of measurement data with databases mineral of samples extracted from iron sand using strong magnets

Measurement data			Mineral Database			Types of minerals	Crystal System	D (nm)
2 θ (°)	d[Å]	I _r (%)	2 θ (°)	d[Å]	I _r (%)			
21.979	4.044	38.16	21.078	4.212	0.1	Ilmenite	Rhombohedral	90.38
23.757	3.750	9.73	23.757	3.734	24.6	Ilmenite	Rhombohedral	63.48
26.736	3.335	23.81	26.637	3.343	100	Quartz	Hexagonal	159.65
28.083	3.178	100	28.220	3.159	100	Quartz	Hexagonal	160.11
30.142	2.966	4.75	30.228	2.954	28.4	Magnetite	Cubic	20.10
35.645	2.518	18.88	35.606	2.519	100	Magnetite	Cubic	108.73
42.568	2.120	9.49	42.448	2.127	3.9	Quartz	Hexagonal	111.09
50.901	1.795	4.5	50.614	1.818	0.5	Quartz	Hexagonal	57.32
68.092	1.377	2.19	68.306	1.370	6.2	Quartz	Hexagonal	23.42

Table 5. Comparison of measurement data with databases mineral of samples extracted from iron sand using weak magnets

Measurement data			Mineral Database			Types of minerals	Crystal System	D (nm)
2 θ (°)	d[Å]	I _r (%)	2 θ (°)	d[Å]	I _r (%)			
21.906	4.057	30.6	21.910	4.032	21.0	Ilmenite	Rhombohedral	42.60
26.617	3.481	100	26.619	3.473	100	Ilmenite	Rhombohedral	53.18
27.807	3.208	30.05	27.895	3.213	100	Hematite	Rhombohedral	26.66
30.217	2.958	21.75	30.136	2.945	29.3	Magnetite	Cubic	40.21
35.517	2.528	63.76	35.656	2.427	75.0	Hematite	Rhombohedral	54.34
43.102	2.099	13.48	43.142	2.091	20.7	Magnetite	Cubic	41.73
54.271	1.690	10.19	54.125	1.604	47.5	Hematite	Rhombohedral	58.15
57.025	1.615	14.45	57.056	1.605	27.6	Magnetite	Cubic	58.90
62.677	1.482	14.73	62.657	1.471	35.0	Magnetite	Cubic	45.44

The magnetic mineral types found in the extraction results were shown by the XRD measurements on the PNT-A06 sample at a depth of 30-35 cm using a strong magnet (Table 4). The iron sand with an angle of 2θ of 30.142° , and 35.645° with $d[\text{\AA}]$ spacing of 2.966\AA , and 2.518\AA with the relative intensity obtained from measurement results known that 4.75% and 18.88% are minerals Magnetite with lattice parameters $a=b=c=8.356 \text{\AA}$; $\alpha=\beta=\gamma=90^\circ$. Meanwhile, the minerals at an angle (2θ) of 21.089° , and 23.757° are known to minerals Ilmenite with $d[\text{\AA}]$ spacing of 4.044\AA and $3.745.4 \text{\AA}$ having lattice parameters $a=b=5.100 \text{\AA}$ and $c = 13.978 \text{\AA}$; $\alpha=\beta=90^\circ$ and $\gamma=120^\circ$ with space group R-3 with a Hexagonal structure having a relative measurement intensity of 38.16%, and 9.73%. Other types of minerals that can be seen at the diffraction angle (2θ) of 26.736° , 28.190° , 42.568° , and 50.701° namely Quartz show non-magnetic minerals that are known to be with the most significant intensity reaching 100%. Thus the diffractogram analysis shows that the types of minerals that make it up iron sand are Magnetite (Fe_3O_4) and Ilmenite (FeTiO_3).

There are still many non-magnetic minerals, such as quartz, based on the results of XRD measurements using weak magnets, so weak magnets are used to obtain magnetic minerals. The results of the measurements were matched to mineral databases (Table 5) shows the existence of magnetic mineral content in an iron sand extraction sample with the known angular intensity of 2θ which is 35.518° , and 54.272° is a Hematite mineral with lattice parameters $a=b=5.032 \text{\AA}$, and $c=13.733 \text{\AA}$; $\alpha=\beta=90^\circ$, and $\gamma=120^\circ$ with space group R-3c with a Rhombohedral structure, while the angular intensity of 2θ is found at 30.217° , 43.102° , 57.025° , and 62.678° , the minerals obtained are Magnetite with lattice parameters $a=b=c=8.380.8 \text{\AA}$; $\alpha=\beta=\gamma=90^\circ$. And with an angular intensity of 2θ found at $27,806^\circ$, and $26,616^\circ$, the known mineral is Ilmenite. Strong magnets had an average crystal size of 88.25 nm, while weak magnets had an average crystal size of 46.80 nm. As a result, extraction with a weak magnet produced more dominant magnetic minerals, like Magnetite (Fe_3O_4), Hematite ($\alpha\text{-Fe}_2\text{O}_3$), and Ilmenite (FeTiO_3)^[30,31].

c. PNT20-0616-1-B10 0-5 cm

1) Measurement data of iron sand extraction samples using strong and weak magnets The

The samples from the iron sand extraction of PNT area sample B01 were measured using XRD at a depth of 0-5 cm, yielding a diffractogram (Figure 7) with some peaks visible. Mineral kinds are recognized using the diffraction angle (2θ), and the distance of fields (d), with magnetic and nonmagnetic minerals being recognized by comparing measurement techniques such as data mineral database.

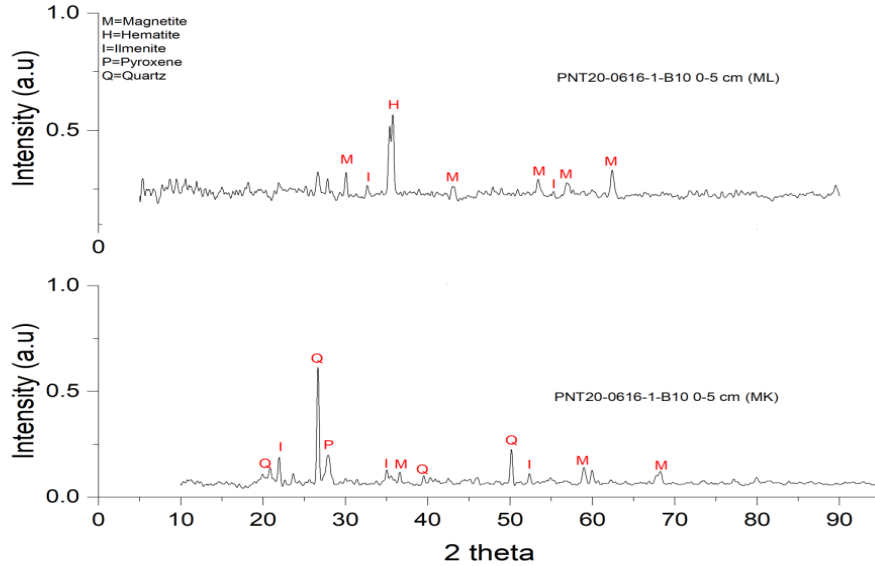


Figure 7. measurement results of XRD samples extracted from iron sand using strong and weak magnets in the PNT region at a depth of 0-5 cm

Table 6. Comparison of measurement data with database mineral sample results. Extraction of iron sand using strong magnets

Measurement data			Mineral Database			Types of minerals	Crystal System	D (nm)
2θ(°)	d[Å]	I _r (%)	2θ(°)	d[Å]	I _r (%)			
20.850	4.261	11.4	20.861	4.255	14.4	Quartz	Hexagonal	78.93
23.642	3.763	7.83	23.617	3.764	33.7	Ilmenite	Rhombohedral	105.76
26.683	3.341	100	26.642	3.430	100.0	Quartz	Hexagonal	106.39
27.794	3.210	16.17	27.670	3.221	21.8	Pyroxene	Orthorhombic	79.97
34.991	2.564	18.2	34.967	2.564	33.7	Ilmenite	Rhombohedral	216.93
36.600	2.455	10.9	36.686	2.448	100.0	Magnetite	Cubic	217.92
39.517	2.281	6.26	39.470	2.281	9.3	Quartz	Hexagonal	54.99
50.132	1.820	26.36	50.624	1.802	0.5	Quartz	Hexagonal	137.14
52.318	1.749	6.24	52.611	1.748	25.0	Ilmenite	Rhombohedral	69.20
59.920	1.544	7.58	59.083	1.562	24.0	Magnetite	Cubic	71.69
68.262	1.374	6.8	68.300	1.372	1.0	Magnetite	Cubic	62.52

Table 7. Comparison of measurement data with databases mineral of samples extracted from iron sand using weak magnets.

Measurement Data			Mineral Database			Types of Minerals	Crystal System	D (nm)
2θ(°)	d[Å]	I _r (%)	2θ(°)	d[Å]	I _r (%)			
30.077	2.9712	23.28	30.120	2.960	29.5	Magnetite	Cubic	26.78
32.620	2.7451	14.67	32.512	2.710	100.0	Ilmenite	Rhombohedral	53.92
35.785	2.5093	100.00	35.744	2.510	50.0	Hematite	Rhombohedral	54.39
43.006	2.1032	12.12	43.118	2.090	20.6	Magnetite	Cubic	33.37
53.422	1.7151	19.86	53.493	1.710	8.3	Magnetite	Cubic	57.93
62.405	1.4881	31.67	62.620	1.480	35.2	Magnetite	Cubic	60.50
73.694	1.2856	3.4	73.762	1.284	0.3	Ilmenite	Rhombohedral	32.33

The results of XRD measurements showed the types of magnetic minerals found in the extraction findings on the PNT-B10 sample at a depth of 0-5 cm. The diffraction angle of 2θ is found at peaks of 36.600° , 59.920° , and 68.261° with distances between d [\AA] of fields 2.455\AA , 1.544\AA , and 1.374\AA , namely minerals Magnetite with relatively low intensity obtained from the measurement results are 10.9%, 7.58%, and 6.8% with the grid parameters are $a=b=c=8.118\text{\AA}$; $\alpha=\beta=\gamma=90^\circ$. Meanwhile, the minerals that are known at the diffraction angle at the peaks of 23.642° , 34.991° , and 52.318° are minerals Ilmenite with relative measurement intensities of 7.83%, 18.2%, and 6.24% with lattice parameters $a=b=5,128\text{\AA}$ and $c=14,187\text{\AA}$; $\alpha=\beta=90^\circ$ and $\gamma=120^\circ$ with space group R-3 with structure Hexagonal. Other types of minerals that are present at the diffraction angle (2θ) at the peak of 27.794° namely Pyroxene and the diffraction angle (2θ) of 20.850° , 26.683° , 39.517° , and $50,132^\circ$ the known minerals are Quartz which shows non-magnetic minerals and with the most significant intensity reaching 100%. Thus the diffractogram analysis shows that the magnetic minerals that make it up iron sand are Magnetite (Fe_3O_4) and Ilmenite (FeTiO_3).

Based on the results of XRD measurements using strong magnets, there are still many non-magnetic minerals such as quartz, so weak magnets are used to obtain magnetic minerals. The results of the measurements were matched to mineral databases (Table 7), the magnetic minerals that were found in the result of the extraction are known in the intensity of the diffraction angle (2θ) is at the peak $35,785^\circ$ is a mineral Hematite that has a lattice parameter $a=b=5,031\text{\AA}$ and $c=13.737\text{\AA}$; $\alpha=\beta=90^\circ$ and $\gamma=120^\circ$ with space group R-3c with structure Rhombohedral, at diffraction angle intensity (2θ) 30.077° , 43.106° , 53.422° , and 62.505° are Magnetite with lattice parameters of $a=b=c=8.385\text{\AA}$; $\alpha=\beta=\gamma=90^\circ$ with a structure Cubic, while the diffraction angle (2θ) is $32,620^\circ$, and $73,700^\circ$ namely Ilmenite and the lattice parameters $a=b=5.0900\text{\AA}$ and $c=14.0900\text{\AA}$; $\alpha=\beta=90^\circ$ and $\gamma=120^\circ$ with space group R-3 with Rhombohedral structure. Strong magnets had an average crystal size of 109.22 nm, while weak magnets had an average crystal size of 45.60 nm. Therefore Extraction using a weak magnet obtained magnetic minerals that are more dominant, namely Magnetite (Fe_3O_4), Hematite (Fe_2O_3), and Ilmenite (FeTiO_3)^[32,33].

CONCLUSION

Based on the results of measurements compared to databases a mineral was generated using XRD. The types of minerals, crystal structure, and crystal size of Pasia Nan Tigo Beach's iron sand can be seen. The content Magnetite (Fe_3O_4) with a Cubic structure, Hematite ($\alpha\text{-Fe}_2\text{O}_3$) with a Hexagonal structure, and Ilmenite (FeTiO_3) with a Hexagonal structure are kinds and structures of magnetic minerals found in samples retrieved from iron sand using powerful magnets. Magnetite (Fe_3O_4) with a Cubic structure, Hematite ($\alpha\text{-Fe}_2\text{O}_3$) with a Rhombohedral structure, and Ilmenite (FeTiO_3) with a Rhombohedral structure all use a weak magnet. Meanwhile, the non-magnetic mineral identified, Quartz (SiO_2) performs the role of even an impurity. PNT-B01 0-5 cm has an average crystal size of 100.85 nm and a weak magnet of 49.36 nm, sample PNT-A06 30-35 cm has an average crystal size of 88.25 nm and a weak magnet of 46.80 nm, and sample PNT-B10 0-5 cm has an average crystal size of 109.22 nm and a weak magnet of 45.60 nm.

ACKNOWLEDGMENTS

The UNP Research and Service Institute funded the Applied Research plan with contract number 1617/ UN35.13/LT/2020, which the author gratefully acknowledges.

REFERENCES

- 1 Karimah & Irjan, I. 2020. Investigation The prospect of Iron Sand in Sungai Topo Hamlet, Sungai Teluk Village, Sangkapura District, Gresik Regency using the Magnetic Method. *J. Fis. Indonesia*, 22 (1), 17.
- 2 Setiawati, L. D., Rahman, T.P., Nugroho, D.W., Ikono, R., & Rochman, T. 2013. Extraction Of Titanium Dioxide (TiO₂) From Iron Sand Using Hydrometallurgy Method. *Semirata FMIPA Univ. Lampung*, 465–468.
- 3 Mufit Fatni, Satria. B., Harman, Amir., Fadhillah. 2013. Kaitan Sifat Magnetik Dengan Tingkat Kehitaman (Darkness) Pasir Besi Di Pantai Masang Sumatera Barat. *Eksakta*, 2, 70–75.
- 4 Aditia, E. 2019. Making Community Based Rw Profiles in Pasie Nan Tigo Village, Koto Tengah District, Padang City. *J. Abdimas*, 22 (2), 167–178.
- 5 Setianto, B., Santosa, D., Hidayat, & Panatarani, C. 2017. Quantitative Analysis of Mixture of Oxide Compounds as a Basis for Identifying Content of Natural Resources, *Exacta*, 18 (2), 173–177.
- 6 Afdal, A., & Islami, E. N. 2015. Karakterisasi Magnetik Batuan Besi Dari Bukit Barampuang, Nagari Lolo, Kecamatan Pantai Cermin, Kabupaten Solok, Sumatera Barat. *SEMIRATA*, 2(1).
- 7 Afdal, A. 2013. Characterization of Magnetic Properties and Mineral Content of Iron Sand in the Batang Kuranji River Padang, West Sumatra. *J. Fis.Univ. Andalas*, 5 (1), 24–30.
- 8 Muhammad, A., Halim, Y., Urrilijanto, U., & Manaf A, 2000. Early studies on the development of iron sand for the coast of Aceh as a raw material for the manufacture of magnetic materials. *Pros. Simp. Fis. National, Puspiptek-Serpong*, 25–27.
- 9 Rifai, H., Erni, & Irvan, M. 2010. Magnetic Extraction of Methanol-Soap Bathed Muds. *J. Researchers. Science*, 14, 25–28.
- 10 Irvan, M., Bijaksana, S., & Hamdi, H. 2010. Identifikasi Mineral Magnetik Pada Tinta Kering (Toner). *EKSAKTA*, 2. 32-39.
- 11 Mürbe, A. Rechtenbach, & Töpfer, J. 2008. Synthesis and physical characterization of magnetite nanoparticles for biomedical applications. *Mater. Chem. Phys.*, 110 (2–3), 426–433.
- 12 Minaei, S. E., Khoei, S., Khoei, S., Vafashoar, F., & Mahabadi, V. P. 2019. In vitro anti-cancer efficacy of multi-functionalized magnetite nanoparticles combining alternating magnetic hyperthermia in glioblastoma cancer cells. *Mater. Sci. Eng. C*, 101, 575–587.
- 13 Yew, Y. P., Shameli, K., Miyake, M., Khairudin, N. B. B. A., Mohamad, S. E. B., Naiki, T., & Lee, K. X. 2020. Green biosynthesis of superparamagnetic magnetite Fe₃O₄ nanoparticles and biomedical applications in targeted anticancer drug delivery system: A review. *Arab. J. Chem.*, 13 (1), 2287–2308.
- 14 Shinde, S. S., Bansode, R. A., Bhosale, C. H., & Rajpure, K. Y. 2011. Physical properties of hematite α -Fe₂O₃ thin films: Application to photoelectrochemical solar cells. *J. Semicond.*, 32 (1), 1–8.
- 15 Yulianto, A., Sulhadi, S., Azis, A. L. I., & Dayati, E. 2013. Synthesis of iron sand into nano Mn-ferrite. *Malaysian Journal of Fundamental and Applied Sciences*, 9(4). 1-6.
- 16 Prasetyo, A. B., Prasetyo, P., & Matahari, I. 2014. Making α -Fe₂O₃ from Iron Ore Processing Hematite Type Primer For Lithium Battery Raw Material. *Maj. Metal.*, 179–189.
- 17 Yulianto, A., Bijaksana, S., Loeksmanto, W., & Daniel, K. 2003. The production of hematite (α -Fe₂O₃) from iron sand utilizes natural potential as an industrial material based on magnetic properties. *Journal of Science Indonesian Material*, 5 (1). 51–54.

- 18 Dearing, J. 1999. *Environmental Magnetic Susceptibility: Using the Bartington MS2 System*. British Library Cataloging in Publication Data.
- 19 Rifai, H., Putra, R., Fadila, M. R., Erni, E., & Wurster, C. M. 2018. Magnetic Susceptibility and Heavy Metals in Guano from South Sulawesi Caves. *IOP Conf. Ser. Mater. Sci. Eng.*, 335 (1).
- 20 Sasmita, A., Rifai, H., Putra, R., Aisyah, N., Phua, M., Eisele, S., Forni, Francesca., & de la Maisonneuve, C. B. 2020. Identification of magnetic minerals in the peatlands cores from Lake Above West Sumatra, Indonesia. *J. Phys. Conf. Ser.*, 1481 (1).
- 21 Rusli, N. G. D., Hamdi, & Mufit, F. 2014. The Relationship between the Composition of Basic Elements of Magnetic Minerals and the Magnetic Susceptibility Value of Guano from Bau-Bau Cave, East Kalimantan. *Pillar Phys.*, 4, 49–56.
- 22 Putra, R., Rifai, H., & Wurster, C. M. 2019. Relationship between magnetic susceptibility and elemental composition of Guano from Solek Cave, West Sumatra. *J. Phys. Conf. Ser.*, 1185 (1).
- 23 Jahidin, Ngkoimani, L. O., & Bijaksana, S. 2011. Analisis Suseptibilitas Magnetik Batuan Ultrabasa di Desa Mosolo Pulau Wawonii Provinsi Sulawesi Tenggara. *Paradigma*. 15(2). 105-112
- 24 Aji, M. P., Yulianto, A., & Bijaksana, S. 2007. Synthesis Nano Particles Magnetite, Maghemite and Hematite from Local Materials. *J. Mater Science. Indonesia.*, 106–108.
- 25 Haryani, H., & Utama, L. 2016. Revitalization Of Coastal Area Pasie Nan Tigo Padang City For Hazard Mitigation. *MIMBAR: Jurnal Sosial dan Pembangunan*, 32(1), 49-57.
- 26 Mukhriani. 2014. Extraction, Separation Of Compounds, And Identification Of Active Compounds. *J. Kesehat.*, 7 (2).
- 27 Cullity, B. D. 1956. *Elements of X-ray Diffraction*. Addison-Wesley Publishing.
- 28 Afriyeni, P., Rifai, H., Maisonneuve, C. B., Forni, F., Eisele, S., Phua, M., & Putra, R. 2020. Identification of magnetic minerals in peatland at the section of DD REP B 693 lake Above using XRD (X-ray Diffraction). *J. Phys. Conf. Ser.*, 1481 (1), 1-7.
- 29 Pertama, D. Y. 2014. Identification of Guano Magnetic Mineral Types from Bau-Bau Cave, East Kalimantan, using x-ray diffraction (XRD). *Pillar Of Physics*, 4(2), 25–31
- 30 Dewi, S. H. & Adi, W. A. 2018. Synthesis and characterization of high purity Fe₃O₄ and α - Fe₂O₃ from local iron sand. *J. Phys. Conf. Ser.*, 1091 (1), 0–9.
- 31 Puspitarum, D. L., Safitri, G., Ardiyanti, H., & Anrokhi, M. S. 2019. Characterization And Nature Of Iron Sand In The Central Lampung Region. *J. Educator. Fis.*, 7 (2), 236.
- 32 Yulianto, A., Bijaksana, S., & Loeksmanto, W. 2003. Comparative Study on Magnetic Characterization of Iron Sand from Several Locations in Central Java. *Indones. J. Phys.*, 14 (2), 63–66.
- 33 Fajri, R. N., Putra, R., Afriyeni, P., De Maisonneuve, C., Phua, M., Eisele, S., Forni, Francesca., & Rifai, H. 2020. Analyzing magnetic susceptibility and elemental composition of rocks and soil around Lake Diatas, West Sumatra, Indonesia. *J. Phys. Conf. Ser.*, 1481 (1).